SHEAR-WAVE Q AND ITS FREQUENCY DEPENDENCE IN THE CRUST OF SOUTHEASTERN ASIA FROM SURFACE-WAVE ATTENUATION

Alemayehu L. Jemberie and Brian J. Mitchell

Saint Louis University

Sponsored by Defense Threat Reduction Agency

Contract No. DTRA-01-00-C-0213

ABSTRACT

Models of shear-wave Q (Q_μ) have been obtained for the crust over a broad region of southeastern Asia, including China and portions of surrounding countries, using a single-station multi-mode method. Event and station coverage is sufficient to allow the mapping of Q_μ variations for three depth ranges in the crust and, in some sub-regions, the uppermost mantle. In layer 1 (10 km thick) Q_μ is highest in southeastern China, where it attains values of about 250. These values are consistent with the relatively high values of Lg coda Q found in earlier work. Q_μ decreases from east to west and reaches a minimum of about 40 in parts of western China, including part of the Tibetan Plateau. Further west, Q_μ increases in a region that comprises the Tarim Basin and parts of southwestern China. Layer 2 (20 km thick) exhibits highest values of Q_μ (140) in eastern China and lowest values (about 60) in the eastern portion of the Tibetan Plateau and in southernmost central China (about 80). A band of relatively high values (with a minimum of about 140) lies between those two regions and extends northward to Mongolia. Layer 3 (30 km thick) contains a concentrated zone of high Q values (up to 200) in north-central China and another (with values up to 160) in northwestern China. They are separated by a north-south band of lower Q_μ values (about 100).

We have computed Q at 1 Hz (Q_o) and the value of frequency dependence (η) that would be predicted by shear-wave models in various sub-regions of southeastern Asia and compared them to previously measured values of Lg coda Q and their frequency dependence in the same regions. For most cases, in order to match predicted and observed values, shear-wave frequency dependence values between 0.0 and 0.6 are required. For most sub-regions adequate agreement can be achieved by assuming the η is constant with depth, but a few cases suggest a depth-variable η.

OBJECTIVE

Q values for seismic shear waves (Q_μ) that propagate in the crust are known to vary laterally by as much as an order of magnitude or more (Mitchell, 1995) and to vary with frequency at least at frequencies near 1 Hz and higher (Mitchell, 1980). Differences in Q_μ will produce path-dependent amplitudes and waveforms for regional phases. If the Q variations are large enough and are not corrected for, magnitude and moment estimates for regional events could be greatly in error. If Q is very low in a region, small signals may be lost in noise and events that generated them could go undetected when epicentral paths are too great. Moreover, if depth variations of Q_μ differ from those assumed to occur, discrimination studies that use amplitude ratios for regional phases that travel predominantly at different depths could give incorrect results.

Our objectives are (1) to use seismic surface waves to determine depth-dependent regional variations of Q_μ over distances that are as small as possible, and (2) to estimate frequency dependence values (ζ) for Q_μ that explain the attenuation observed for surface waves at intermediate periods (about 5-50s) and values of Q_o (Q_{Lg} at 1 Hz) and η (the frequency dependence of Q_{Lg} at 1 Hz). This information will allow us to extend our results on regional variations of Q_μ using surface waves to frequencies that are important for regional phases.

RESEARCH ACCOMPLISHED

The method used in our research requires Rayleigh waves that have traveled over regional distances between seismic events and stations and that have not been greatly affected by major lateral variations in velocity structure. We investigated the spectra for all events that occurred in our region of study between 1990 and 1999 and found 34 that provided useful spectra for our research. They were recorded at one or more of the 13 seismic stations in our region of study and had magnitudes between 4.9 and 6.2. Figure 1 shows locations for events and stations used in the study as well as paths between them. The paths range in distance between 300 and 3000 km and cover a region that extends between about 25 and 55 degrees north latitude and between about 60 and 130 degrees east longitude.

Our method matches theoretically predicted fundamental-mode and higher-mode Rayleigh-wave spectra computed for sources with known depths, moments, and focal mechanism solutions with the corresponding observed spectra. The theoretical spectral were computed using the equations of Anderson *et al* (1965). We used fundamental mode spectra at periods between about 5 and 50 s and higher mode spectra, consisting of super-positions of many individual higher modes, at periods between about 3 and 10 s. We assumed an initial Q model and adjusted it until a good fit was achieved between theoretical and observed spectra. We initially tried to use published focal depths and moments in our computations, but we sometimes had to adjust the values of those parameters to obtain a good fit. We started our spectral fitting process by varying values of Q_μ in layer 1, which we took to be 10 km thick, and holding Q_μ at greater depths at high values. We found a value of Q_μ that provided the best possible agreement in the short-period portion of the theoretical and observed spectra. We then held Q_μ in layer 1 at the derived value and adjusted Q_μ in layer 2 to obtain the best spectral fit at longer periods for the fundamental Rayleigh mode. Fixing Q_μ in both layers 1 and 2, we then determined Q_μ in layer 3 in the same way.

Figure 2 exhibits comparisons between observed and theoretical for nine paths. About half of them show that theoretical and observed spectra agree well for the fundamental mode over the entire period range but for others the observed spectra are higher than those observed at periods greater than 20 or 30 s. This can be attributed to low signal/noise ratios at the longer periods. In these nine examples Q_μ in layer 1 varies between 55 and 150, Q_μ in layer 2 varies between 40 and 120, and Q_μ in layer 3 varies between 80 and 200. Figure 3 shows the models that were obtained by the spectral fits for the same nine sets of spectra. The standard deviations for the Q_μ values in each layer were obtained using the method described by Cheng and Mitchell (1981). The method adapts the equation of Anderson *et al* (1965) to error estimation using rms misfits between theoretical and observed spectra. The models exhibit wide variations in Q_μ values in all three layers and in the nature of Q_μ depth variation; Q_μ sometimes increases and sometimes decreases with depth.

Figures 4-6 map Q_μ variation for the three depth ranges chosen for our study. For layer 1 the highest values (as high as 240) correspond to a stable region that is termed the Southeast China Block and lowest values (40-60) correspond to the Tibetan Plateau and adjacent regions, as well as to a region near the Baikal Rift. A second region of relatively high Q_μ values lies in western Mongolia and southernmost Siberia at longitudes between about 90^o and 100^o. There are three centers of low Q_μ in layer 2, one in the southern portion of the Tibetan Plateau, one centered in northern

Myanmar and southernmost China, and one in the region of the Baikal Rift. High values extend from central China to southeastern-most Siberia. Since error bars for many of our Q_μ models indicate that large uncertainties characterize layer 3, we consider only broad-scale variations to be significant. Relatively high values underlie Mongolia and the Baikal Rift, and small regions of southern China, and western-most China.

Almost all mechanisms that explain variations of Q_μ in the Earth predict that Q_μ should vary with frequency (e.g. Jackson and Anderson, 1970). This frequency dependence has been observed in laboratory experiments and has been required to simultaneously explain measured Q_μ values for free oscillations of the Earth and for 1-Hz body waves. It is also required to simultaneously explain the attenuation of Rayleigh waves at intermediate periods (5-100s) and Lg waves at 1 Hz. It is important to determine frequency dependence values for Q_μ for frequency ranges that are important in monitoring the Comprehensive Nuclear-Test-Ban treaty. If this can be determined we will be able to extrapolate values of Q determined from surface waves to the higher frequencies that characterize regional phases at shorter distances.

As a first step toward determining the frequency dependence of Q_μ and how it may vary with depth we wave developed a method by which the frequency dependence can be obtained for our crustal models using a combined forward modeling/formal inversion procedure. It is a variation of a previously developed procedure (Mitchell and Xie, 1994) and obtains a frequency dependence value that reconciles Q_μ values at 1 Hz with those obtained at surface-wave periods (5-50s). The process proceeds as follows:

1. Compute attenuation coefficients for the fundamental Rayleigh mode, as a function of period, for the three-layer Q_μ model and corresponding velocity model of interest.

2. Assume a depth distribution for the frequency dependence, ζ, of Q_μ and determine the attenuation coefficients obtained in step 1 to obtain a Q_μ model.

3. Calculate the fundamental-mode Rayleigh-wave attenuation coefficient values which are predicted by the model from step 2 and compare them with the values of step 1. An example appears in Figure 7. If they agree within reasonable uncertainties go to step 4; if not, try a new distribution of ζ.

4. Compute synthetic Lg seismograms at several distances from a seismic source using the appropriate velocity and Q_μ models from step 2.

5. Apply the stacked spectral ratio (SSR) method of Xie and Nuttli (1998) to the set of synthetic seismograms in step 4 to obtain values of Q_o and η predicted by the derived Q_μ model and compare them with measured values from maps of Eurasia (Mitchell *et al*, 1997).

6. If necessary, change the depth distribution of ζ in step 2 and go through the procedure again.

7. From the results of step 5, compute Q_μ at frequencies of interest (1 Hz for the present study).

Four examples of results using this procedure appear in Figure 8. The solid lines in the left-hand side of each pair of boxes are frequency-independent Q_μ models obtained from spectral matching and the dashed lines show models at 1Hz using our procedure to obtain Q_μ frequency dependence. The boxes on the right-hand side of each pair show the assumed distributions of ζ with depth. In all but one of the examples, a constant value of ζ produced acceptable results. Values of Qo and η predicted by the models for Lg attenuation at 1 Hz appear below each set of models. Note that, as shown by the model on the upper left of the figure, a model with frequency-independent Q_μ can still produce a frequency-dependent Q value for Lg if Q_μ increases rapidly at mid-crustal depths. This phenomenon was shown to occur in the crust of the Basin and Range province of the United States (Mitchell, 1991).

CONCLUSIONS AND RECOMMENDATIONS

Three-layer models of shear-wave Q (Q_μ) have been obtained for a broad portion of southeastern Asia. Layer 1 extends through the upper 10 km of the crust, layer 2 through the depth range 10-30 km, and layer 3 through

30-60 km. The models therefore include the uppermost mantle in some regions, but in the Tibetan Plateau correspond only to the crust. Values of Q_μ in layer 1, from a frequency-independent determination, vary between 55 and 150, are lowest in the Tibetan Plateau and highest in the Southeast China Block. A zone of relatively high Q_μ lies in western Mongolia and southern Siberia. In layer 2 Q_μ varies between 40 and 120 and contains three centers of low values, one in the southern part of the Tibetan Plateau, one centered in northern Myanmar and southernmost China, and one near the Baikal rift. High values extend through much of central and eastern China and southeastern Siberia. Only the broad-scale variation Q_μ are taken to be significant and vary between 80 and 200 with relatively high values underlying Mongolia and the Baikal Rift, and beneath small portions of southern and westernmost China.

Frequency-dependent models of Q_μ were obtained that explain both the observed attenuation of fundamental-mode Rayleigh waves and measured values of Lg coda Q. Variations of the frequency-dependence parameter (ζ) for Q_μ vary between 0.0 and 0.6. Both this Q_μ frequency dependence and the depth distribution of Q_μ values contribute to values of the frequency dependence (η) of Q_{Lg}.

ACKNOWLEDGEMENTS

Lianli Cong, now at Yunnan University, wrote the programs for plotting amplitude spectra and Robert Herrman developed the code for their computation.

REFERENCES

Anderson, D.L., A. Ben-Menahem and C.B. Archambeau (1965), Attenuation of seismic energy in the upper mantle, *J. Geophys. Res*., **70**, 1441-1448.

Chen, C.C., and B.J. Mitchell (1981), Crustal Q structure in the United States from multi-mode surface waves, *Bull. Seism. Soc. Am.,* **71**, 161-181.

Cong, L., and B.J. Mitchell (1998), Seismic velocity and Q structure of the Middle Eastern crust and upper mantle from surface-wave dispersion and attenuation, *Pure App. Geophys*., **153**, 503-538.

Jackson, D.D., and D.L. Anderson (1970), Physical mechanisms for seismic wave attenuation, *Rev. Geophys.,* **8**, 1-63.

Mitchell, B.J. (1980), Frequency dependence of shear wave internal friction in the continental crust of eastern North America, *J. Geophys. Res.,* **85**, 5212-5218.

Mitchell, B.J. (1991), Frequency dependence of QLg and its relation to crustal anelasticity in the Basin and Range province, *Geophys. Res. Lttrs*., **18**, 621-624.

Mitchell, B.J. (1995), Anelastic structure and evolution of the continental crust and upper mantle from seismic surface wave attenuation, *Rev. Geophys*. **33**, 441-462.

Mitchell, B.J., Y. Pan, J. Xie and L. Cong (1997), Lg coda Q variation across Eurasia and its relation to crustal evolution, *J. Geophys. Res*., **102**, 22767-22779.

Xie, J., and O.W. Nuttli (1988), Interpretation of high-frequency coda at large distances: Stochastic modeling and method of inversion, *Geophys. J*., **95**, 579-595.

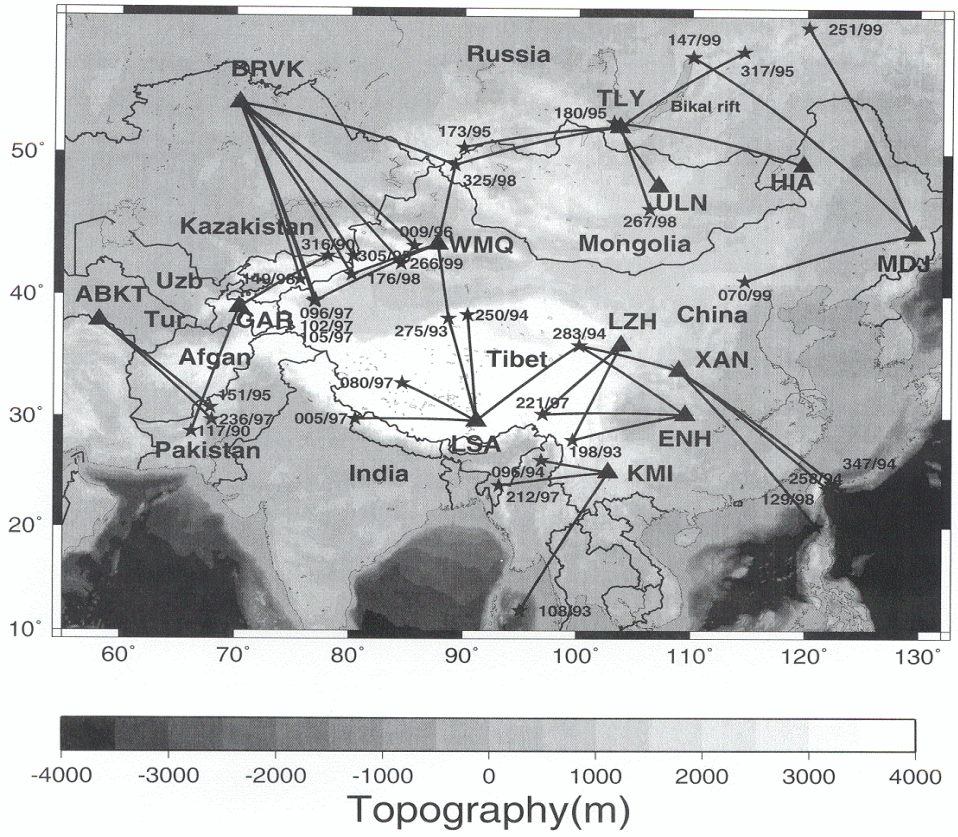

Figure 1. Map of southeastern Asia showing events (stars), stations (triangles), and paths between them.

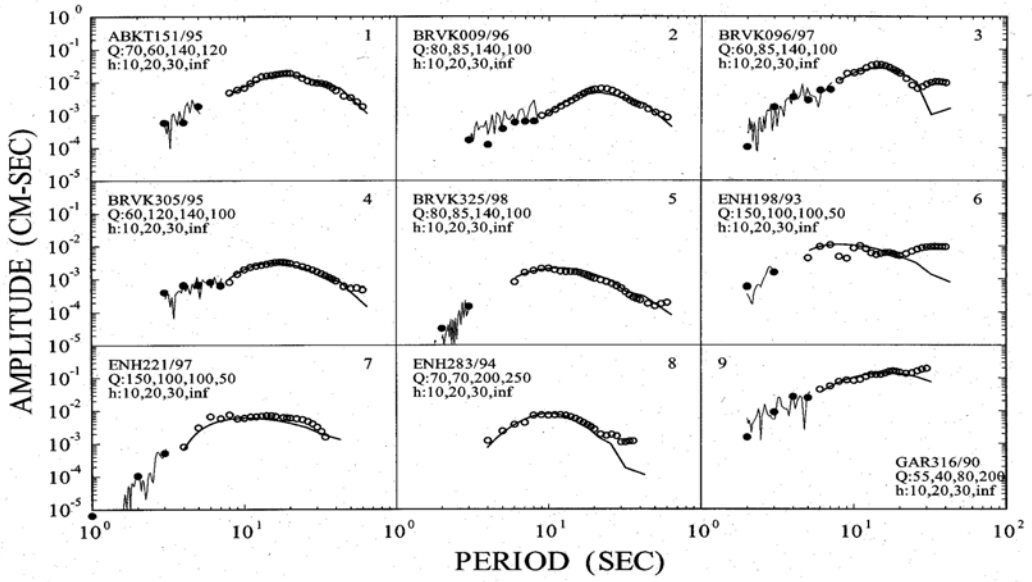

Figure 2. Comparison of theoretical and observed amplitude spectra for nine event-station paths. Open circles denote spectra for fundamental mode spectra and solid circles denote spectra for a superposition of higher modes. The notation in each box gives the station name and event date (in julian day), shear-wave Q values, for three layers and the underlying half-space, and the thicknesses of the layers.

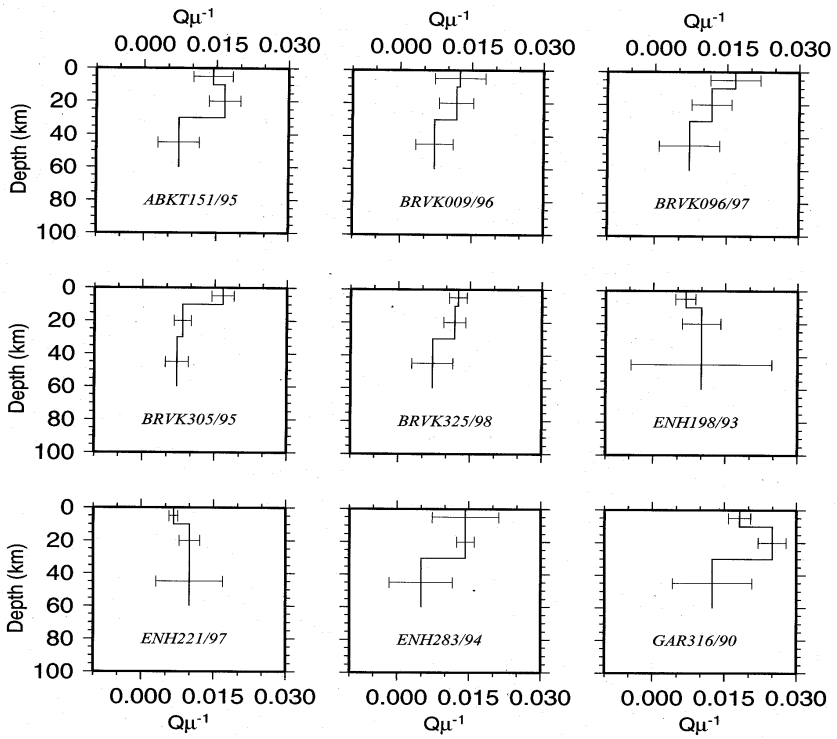

Figure 3. Three-layer models of shear-wave Q with error estimates derived from the spectral matching technique and the spectra of Figure 2.

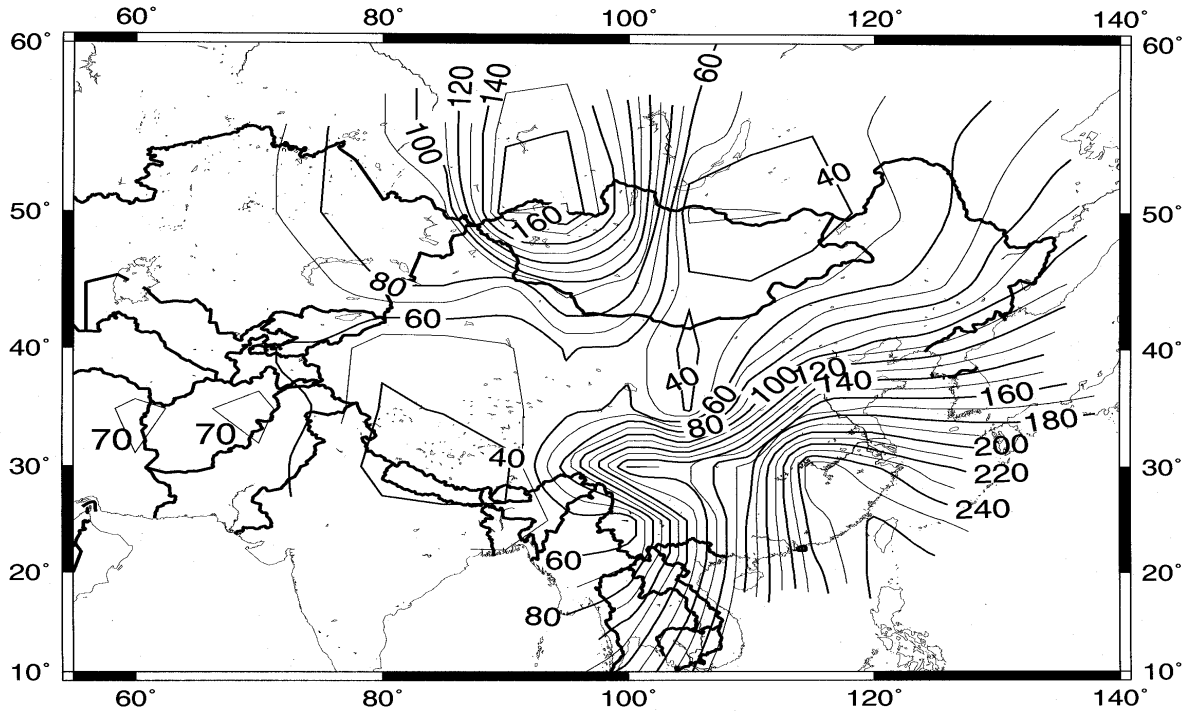

Figure 4. Map of shear-wave Q variations in layer 1 (10 km thick).

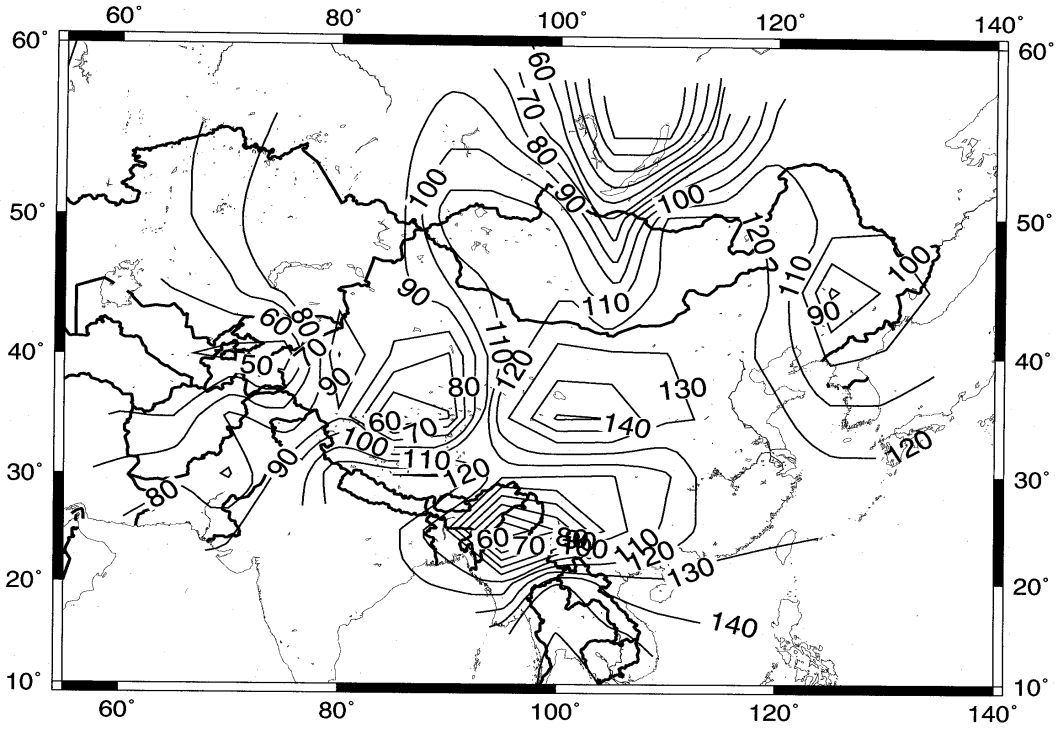

Figure 5. Map of shear-wave Q variations in layer 2 (20 km thick).

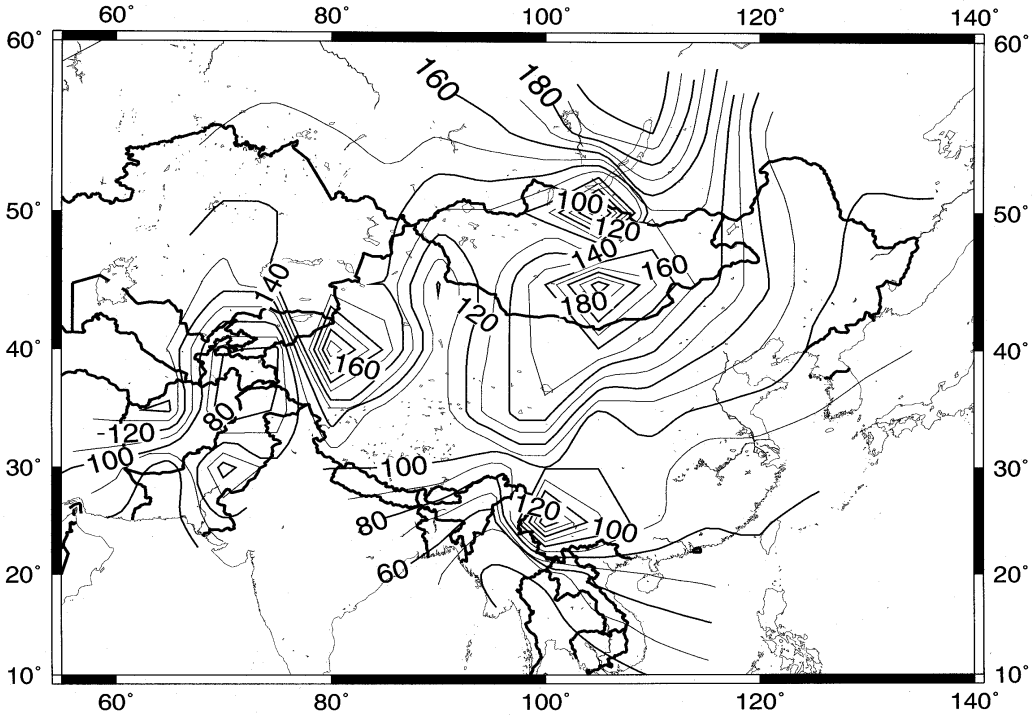

Figure 6. Map of shear-wave Q variations in layer 3 (30 km thick).

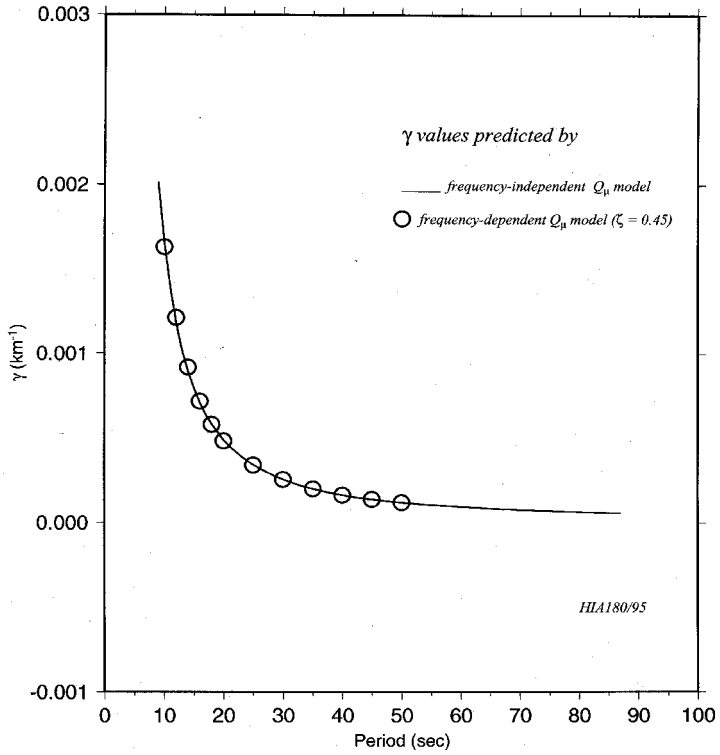

Figure 7. Comparison of Rayleigh-wave attenuation coefficients predicted by the three-layer frequency-independent model of shear-wave Q with a frequency-dependent model for spectra obtained at station HIA for the event of day 180 in 1995.

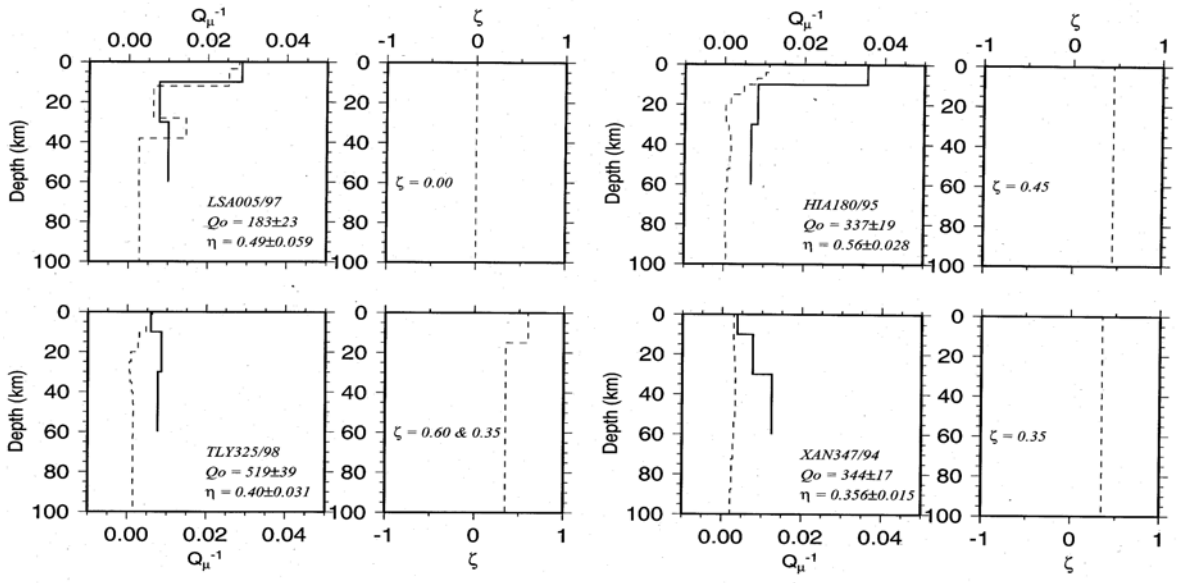

Figure 8. Comparison of frequency-independent (solid lines) and frequency-dependent (dashed lines) models of shear-wave Q for four cases obtained for the ς distribution plotted next to each pair of models. Values of Q_o and η for Q_{Lg} at 1 Hz predicted by the models are given for all cases.